Antiviral Research 170 (2019) 104567

Contents lists available at ScienceDirect

Antiviral Research

journal homepage: www.elsevier.com/locate/antiviral

Polyphenylene carboxymethylene (PPCM) in vitro antiviral efficacy against Ebola virus in the context of a sexually transmitted infection

Olivier Escaffre[a,*], Terry L. Juelich[a], Alexander N. Freiberg[a,b,c,**]

[a] Department of Pathology, Galveston, TX, 77555, USA
[b] Center for Biodefense and Emerging Infectious Diseases, Galveston, TX, 77555, USA
[c] Institute for Human Infections and Immunity, University of Texas Medical Branch, Galveston, TX, 77555, USA

ARTICLE INFO

Keywords:
Ebola virus
Sexually transmitted infections
Polyphenylene carboxymethylene

ABSTRACT

Ebola virus disease (EVD) is caused by Ebola virus (EBOV) and characterized in humans by hemorrhagic fever with high fatality rates. Human-to-human EBOV transmission occurs by physical contact with infected body fluids, or indirectly by contaminated surfaces. Sexual transmission is a route of infection only recently documented despite isolating EBOV virus or genome in the semen since 1976. Data on dissemination of EBOV from survivors remain limited and EBOV pathogenesis in humans following sexual transmission is unknown.

The *in vitro* antiviral efficacy of polyphenylene carboxymethylene (PPCM) against EBOV was investigated considering the limited countermeasures available to block infection through sexual intercourse. PPCM is a vaginal topical contraceptive microbicide shown to prevent sexual transmission of HIV, herpes virus, and bacterial infections in several different models. Here we demonstrate its antiviral activity against EBOV. No viral replication was detected in the presence of PPCM in cell culture, including vaginal epithelial (VK2/E6E7) cells. Specifically, PPCM reduced viral attachment to cells by interfering with EBOV glycoprotein, and possibly through binding the cell surface glycosaminoglycan heparan sulfate important in the infection process. EBOV-infected VK2/E6E7 cells were found to secrete type III interferon (IFN), suggesting activation of distinct PRRs or downstream signaling factors from those required for type I and II IFN. The addition of PPCM following cell infection prevented notably the increase of these inflammation markers. Therefore, PPCM could potentially be used as a topical microbicide to reduce transmission by EBOV-positive survivors during sexual intercourse.

1. Introduction

Ebola virus (EBOV) is an enveloped virus member of the family *Filoviridae* (genus *Ebolavirus*), and the causative agent of Ebola virus disease (EVD) characterized by hemorrhagic fever in humans, with mortality rates ranging from 40% up to 90% (Feldmann et al., 2013; Feldmann and Geisbert, 2011). The current Ebola virus outbreak in the Democratic Republic of the Congo was declared on May 8th, 2018 and is totaling 2408 cases with 67% fatality, as of July 6th, 2019 (WHO, 2018). EVD in humans has been extensively investigated since its first recognition in 1976 in the Democratic Republic of The Congo (Commission, 1978). Although multiple therapeutics and experimental vaccines have been shown to be effective *in vitro* or *in vivo* (Dhama et al., 2018; Madelain et al., 2016), none are currently FDA-approved for human use. However, protective efficacy of the rVSVΔG-ZEBOV-GP vaccine was demonstrated in a ring vaccination trial in Guinea, and Sierra Leone in 2015 (Henao-Restrepo et al., 2015, 2017).

Virus transmission between humans occurs by close contact with bodily fluids, indirectly by contaminated objects and through airborne droplets (Emanuel et al., 2018). However, sexual transmission of Ebola virus was only recently documented during the 2014–2016 outbreak in West Africa. The infectious virus and virus genome were previously isolated in the semen of patients in 1976, 1995, and 2000 (Bausch et al., 2007; Emond et al., 1977; Rodriguez et al., 1999; Rowe et al., 1999), without further investigations because little was known of their infectiousness. Indeed, genomic and epidemiologic data provided evidence in 2015 that at least one fatal case of EVD in Liberia in 2015 was contracted through sexual intercourse from a male survivor (Mate et al., 2015). This provided evidence of EBOV infectivity when present in the semen at least 179 days after the onset of disease. Several follow-up studies have reported virus or virus genome isolation in semen up to 2 years after the onset of disease (Barnes et al., 2017; Christie et al., 2015;

* Corresponding author.
** Corresponding author. Department of Pathology, University of Texas Medical Branch, 301 University Boulevard, Galveston, TX, 77555-0609, USA.
E-mail addresses: olescaff@utmb.edu (O. Escaffre), anfreibe@utmb.edu (A.N. Freiberg).

https://doi.org/10.1016/j.antiviral.2019.104567
Received 4 June 2019; Received in revised form 16 July 2019; Accepted 22 July 2019
Available online 24 July 2019
0166-3542/ Published by Elsevier B.V.

Crozier, 2016; Deen et al., 2017; Etard et al., 2017; Fischer et al., 2017; Keita et al., 2017; Mate et al., 2015; Purpura et al., 2016; Sissoko et al., 2017; Soka et al., 2016; Subtil et al., 2017). Although sexual transmission constitutes a less documented route of infection, it has been likely responsible for at least 4 out of the 8 Ebola outbreak flare-ups reported between 2015 and 2016 (Subissi et al., 2018). A mathematical modelling study looking at the contribution of sexual behavior in virus transmission during the 2014–2016 outbreak (Luo et al., 2019) also shows that controlling this route of infection through abstinence, along with isolating infectious patients, could stop an outbreak. Altogether, data on persistence and shedding of Ebola virus from the semen support the critical need to develop rapid antiviral countermeasures preventing virus transmission during unprotected sexual intercourse. WHO still recommends practicing safer sex for at least 12 months after the onset of symptoms (WHO, 2016), which may be too short based on recent studies on virus genome persistence in body fluids (Fischer et al., 2017).

Microbicides are broad-spectrum antimicrobial compounds, administered vaginally prior to sexual activity with the potential for use either alone or in combination with other physical barrier methods against EBOV in the context of a sexually transmitted infection (STI). These products have the advantage of use by women without the need for approval and cooperation from sexual partners, in contrast to condoms. However, no published data are available regarding the efficacy of microbicides against EBOV.

Polyphenylene carboxymethylene (PPCM) is a small polymer derived from mandelic acid condensation (previously called SAMMA in the literature), and a broadly-acting vaginal microbicide. It has been shown to block HIV, herpesviruses 1 and 2, and bacterial infections (Chang et al., 2007; Herold et al., 2002; Zaneveld et al., 2002) in various models, while having no toxicity on vaginal and cervical cells (Zaneveld et al., 2002) or the vaginal flora (Herold et al., 2002).

This study investigated the antiviral activity of PPCM against EBOV in the context of an STI in human cells. PPCM interfered with EBOV replication in human cervical, and human vaginal epithelial cells. Further investigations of the antiviral activity demonstrate that PPCM binds to EBOV glycoprotein (GP), but may also compete for cell surface glycosaminoglycan heparan sulfate (HS) receptors to impair viral attachment and infectivity. Finally, analysis of the inflammatory response in EBOV-infected vaginal epithelial cells included secretion of type I, II, and III interferon whose secretion could be reduced by PPCM.

2. Material and methods

2.1. Cells, PPCM, and virus

293T (ATCC, CRL-1375), Vero-E6 (ATCC, CRL-1586), Vero (ATCC, CCL-81), HeLa (ATCC, CCL-2), and VK2/E6E7 (ATCC, CRL-2616) cells were purchased from American Type Culture Collection (ATCC). 293T, Vero-E6, Vero, and HeLa cells were grown in DMEM (Gibco/Thermo Fisher Scientific) supplemented with heat-inactivated Fetal Bovine Serum (FBS) (Gibco) at 10%, and 10 mM L-Glutamine (Gibco) at 37 °C, 5% CO_2. Normal VK2/E6E7 cells were grown in Keratinocyte-Serum Free medium (GIBCO-BRL 17005–042) with 0.1 ng/ml human recombinant EGF, 0.05 mg/ml bovine pituitary extract, and additional calcium chloride 44.1 mg/L (final concentration 0.4 mM) at 37 °C, 5% CO_2.

Optimal seeding density (cell viability) of each cell type for 5 days of culture was carried out using tetrazolium dye (MTT) (Sigma) to determine the 50% Cytotoxic Concentration (CC_{50}) of polyphenylene carboxymethylene (PPCM) for each cell type, following the manufacturer's instructions. This corresponds to the typical time EBOV reaches highest replication levels *in vitro*. CC_{50} was calculated by regression analysis.

Polyphenylene carboxymethylene (PPCM) polymer was provided by Yaso Therapeutics Inc. A PPCM stock solution was prepared in phosphate-buffered saline (PBS) at 220 mg/ml and sterile-filtered at 0.2 µm prior use. High, medium, and low PPCM concentrations below the CC_{50} for each cell type were arbitrarily used in the EBOV replication kinetic experiments, EBOV GP-cell binding assays, and virus transduction assay.

Recombinant Zaire Ebola virus expressing eGFP (EBOV-eGFP) was propagated in Vero E6 cells. Virus titers were quantified by plaque assay using Vero E6 cells, as previously described (Bazhanov et al., 2017). Titers were reported as $\log_{10}$ pfu/ml. All infectious work was performed in a biosafety level 4 laboratory (BSL4) at the Galveston National Laboratory, UTMB.

2.2. Virus replication kinetics

Sterile PPCM stock was diluted in the appropriate media to obtain concentrations from 2 mg/ml to 10 µg/ml for Vero cells, 25 to 0.1 µg/ml for HeLa cells, and 500 to 5 µg/ml for VK2/E6E7 cells. Vero, HeLa, and VK2/E6E7 cells were seeded in a 12-well plate format the day prior to infection at 3×10^5, 1.5×10^5, and 1.5×10^5 respectively per well in a 600 µl volume. Cells were treated with PPCM starting either 1 h (h) prior infection and again 1 h post-infection (pre-treatment protocol) or only 1 h post infection (no pre-treatment protocol), followed by daily treatment, 24 h apart, throughout the entire experiment. Media (100 µl) with PPCM, when appropriate, was added daily for the purpose of maintaining treatment with freshly prepared PPCM and to compensate for volume loss (100 µl) by sample collection. Virus contact was performed for 1 h and washed off by 3 (100 µl) PBS lavages in both pre-treatment and no pre-treatment experimental conditions.

2.3. Fluorescence microscopy and image analysis

EBOV-eGFP-infected Vero, HeLa and VK2/E6E7 were directly imaged in the BSL4 laboratory using a fluorescence Olympus IS71 microscope at 10× magnification. Images were analyzed with CellProfiler 3.0.0 (Carpenter et al., 2006; Lamprecht et al., 2007) for automated counting of EBOV-eGFP-infected cells per randomly-selected field of view. Briefly, the IdentifyPrimaryObjects module was used to identify Vero, HeLa, and VK2/E6E7 fluorescent positive cells, with a typical diameter of 8–50 pixels. Cells outside the diameter or touching the border of the image were discarded.

2.4. Real-time (RT)-PCR assay

Total cellular RNA from VK2/E6E7 cells was extracted using TRIzol reagent (Invitrogen/Thermo Fisher Scientific), and then purified using Direct-zol RNA miniprep (Zymo Research), following manufacturer's recommendations. Quantitative reverse transcription (RT)-PCR assays were performed using a single TaqMan MGB probe with two unlabeled oligonucleotide primers (IDT) that recognize the gene sequence corresponding to glycoprotein (GP) of EBOV, and the One-step QuantiFast Probe RT-PCR kit (Qiagen). Quantification of 18S rRNA level was performed with the 18S rRNA gene TaqMan assay reagent (Thermo Fisher Scientific) and used as an endogenous control. Duplicate threshold cycle (Ct) values of each sample were analyzed using the comparative delta-delta Ct method ($2^{-\Delta\Delta Ct}$). Cut-off for EBOV positive samples was determined by using non-positive samples (mock-infected cells) as a reference. Cut-off was set at $\Delta Ct = 18.93$ and 17.92 in mock-infected VK2/E6E7 or Vero cells, respectively (Tables 1 and 2). Note that to be positive for EBOV genome a cell sample must have a lower ΔCt than those aforementioned in the respective cell line. The fold change of GP gene expression was similarly calculated using samples from infected cells without any PPCM treatment as a control, after normalization of values using the housekeeping 18S rRNA gene data. Primer and probe sequences were EBOV-Fwd: TTTTCAATCCTCAACC GTAAGGC, Rev: CAGTCCGGTCCCAGAATGTG, and EBOV-Probe: CAT GTGCCGCCCCATCGCTGC, as previously described (Bazhanov et al., 2017; Trombley et al., 2010). The PCR was performed with 35 cycles.

Table 1
Detection and relative quantification of EBOV GP gene expression in EBOV-infected vaginal epithelial cells.

Sample	Replicate	18s RNA Average Ct	EBOV Average Ct	Cut-off positive samples (Average ΔCt)= 18.93		
No virus-No PPCM	1	13.47	32.66			
	2	13.39	32.31			
	3	13.69	32.37			
				Fold-change compared to cut-off ($2^{-\Delta\Delta Ct}$)	Sample result compared to cut-off	
EBOV-No PPCM	1	14.37	22.88	1368.00	+	
	2	13.31	23.40	458.00	+	
	3	13.56	23.45	527.00	+	
				Fold-change compared to cut-off ($2^{-\Delta\Delta Ct}$)	Sample result compared to cut-off	Fold-change compared to calibrator Virus-No PPCM ($2^{-\Delta\Delta Ct}$). Calibrator (Average ΔCt) = 9.50
EBOV-500 ng/µl PPCM	1	13.87	32.84	0.97	-	NA
	2	14.21	32.86	1.22	+	$1.77\ 10^{-3}$
	3	14.34	33.13	1.10	+	$1.60\ 10^{-3}$
EBOV-50 ng/µl PPCM	1	13.61	32.85	0.81	-	NA
	2	13.90	33.43	0.66	-	NA
	3	13.30	32.50	0.83	-	NA
EBOV-5 ng/µl PPCM	1	13.30	32.41	0.88	-	NA
	2	13.34	32.29	0.99	-	NA
	3	13.97	32.25	1.57	+	$2.27\ 10^{-3}$

+: virus genome positive; -: virus genome negative; NA: non-applicable

2.5. Expression of recombinant soluble His-EBOV-GP and purification of S9 monoclonal antibody (Mab S9)

The pCZaire643His plasmid (Nakayama et al., 2010) encoding a truncated soluble codon-optimized EBOV GP, lacking the transmembrane domain and cytoplasmic tail with a C-terminal histidine (His) tag, was kindly provided by Dr. Ayato Takada (The Hokkaido University Research Center for Zoonosis Control, Japan). Expression of His-EBOV-GP (EBOV GP) was performed as previously described (Nakayama et al., 2010). Briefly, 293T cells were transfected with pCZaire643His plasmid using TransIT LT1 (Mirus). Culture supernatants were harvested 48 h post transfection, clarified, and concentrated. EBOV GP was then purified using a HisPur Cobalt Purification kit (Thermoscientific), and dialyzed against phosphate-buffered saline (PBS) overnight at 4 °C. Successful purification of EBOV GP was confirmed by Western-Blot (SDS-PAGE) using a rabbit anti-GP (IBT #301–015) and the presence of a unique band at about 130 KDa corresponding to GP_1 subunit responsible for cellular attachment.

The S9 hybridoma secreting the neutralizing monoclonal S9 antibody (Mab S9) (Hernandez et al., 2015; Marceau et al., 2014) was kindly provided by Dr. Barry Rockx (Erasmus Medical Center, Rotterdam, Netherlands). Briefly, cells were cultured in DMEM (Gibco/Thermo Fisher Scientific) supplemented with FBS (Gibco) at 10%, and 10 mM L-Glutamine (Gibco) at 37 °C, 5% CO_2. Culture supernatant was collected, clarified through 0.45 µm pore-size filter, and S9 monoclonal antibody (Mab S9) concentrated using Amicon ultra 15 (Millipore). Mab S9 was then purified using Nab Spin kit (ThermoScientific).

2.6. EBOV GP-cell binding assay

Level of EBOV GP binding to cells was assessed as follows: 5 µg of purified EBOV GP was incubated in either 500 µl of basal medium or

Table 2
Detection and relative quantification of EBOV GP gene expression and infectious titer in Vero cell cultures inoculated for 5 days with culture supernatants of EBOV-infected VK2/E6E7 cells.

Inoculum on Vero	Replicate	18s RNA Average Ct	EBOV Average Ct	Cut-off positive samples (Average ΔCt)= 17.92		
No virus-No PPCM	1	14.67	32.18			
	2	14.54	32.79			
	3	15.15	33.15			
				Fold-change compared to cut-off ($2^{-\Delta\Delta Ct}$)	Sample result compared to cut-off	Virus titer in Vero culture supernatants (pfu/ml)
EBOV-No PPCM	1	14.40	16.57	55198	+	$1.6\ 10^{4}$
	2	14.85	18.96	14376	+	$4.0\ 10^{4}$
	3	14.05	13.34	405587	+	$7.0\ 10^{5}$
EBOV-500 ng/µl PPCM	1	14.92	35.91	0.12	-	< LOD
	2	14.20	36.55	0.05	-	< LOD
	3	14.51	35.70	0.10	-	< LOD
EBOV-50 ng/µl PPCM	1	13.97	35.11	0.11	-	< LOD
	2	14.13	35.39	0.10	-	< LOD
	3	14.00	33.91	0.25	-	< LOD
EBOV-5 ng/µl PPCM	1	14.42	22.61	850	+	< LOD
	2	14.73	35.31	0.16	-	< LOD
	3	14.35	22.68	771	+	$4.0\ 10^{2}$

+: virus genome positive; -: virus genome negative; LOD: limit of detection of 10^2pfu/ml.

with diluted PPCM in basal DMEM or Keratinocyte medium for 30 min. The mixture was added to a pellet of 3 to 5 × 10^6 cells for 60 min at 4° C. Cells were centrifuged at 220 g for 3 min and rinsed twice with cold PBS. The cell pellet was resuspended in cold western-blot lysing buffer for 30 min on ice, homogenized, and centrifuged again for 10 min at 13,000 rpm for clarification. PPCM concentrations of 2000, 200 and 20 µg/ml were used for Vero cells, 25, 2.5 and 0.25 µg/ml for HeLa cells, and of 500, 50 and 5 µg/ml for VK2/E6E7 cells.

2.7. Western blot

Cell lysates were prepared from pelleted Vero, HeLa, and VK2/E6E7 cells resuspended in a 1X ice-cold RIPA buffer (Thermo Fisher Scientific) with a protease inhibitor cocktail (Roche), according to the manufacturer's instructions. Cell lysates were then clarified and after estimation of protein content with the Nanodrop (Life technologies), 50µg/sample were boiled in 2x Laemmli buffer and resolved on 8% SDS-PAGE gels. Proteins were transferred onto an Immuno-Blot PVDF membrane (Bio-Rad), and nonspecific binding sites were blocked by immersing the membrane in Tris-buffered saline–0.1% Tween 20 (TBST) containing 5% Bovine Serum Albumin powder (Thermo Fisher Scientific). The membranes were then incubated in TBST 2% BSA with the primary antibodies overnight at 4 °C, followed by incubation with the goat anti-rabbit IgG horseradish peroxidase (HRP)-conjugated secondary antibody (Abcam #7090, d/1000) for 60 min. Primary antibodies were rabbit anti-GP (IBT #301–015, d/1000) and rabbit anti-actin (Cell signaling clone 13E5, d/3000). Proteins of interest were visualized with a SuperSignal West Pico chemi-luminescent reagent (Thermo Fisher Scientific) on a C-DiGit Blot Scanner imaging system (LI-COR Biosciences). For densitometry analysis from the digital images captured on the scanner, background was calculated using the median intensity of pixels in a border around a band and was subtracted from the background of that band of interest. Normalization of GP_1 amount was performed using the internal actin loading control.

2.8. Production of recombinant MLV pseudotyped with EBOV GP and transduction assay

Rescue of the recombinant replication-defective Moloney Murine Leukemia Virus pseudotyped with EBOV glycoprotein (MLV-Ebola) was done as previously described (Wool-Lewis and Bates, 1998) with minor changes. The Strawberry reporter gene was packed in MLV-Ebola to assess its level of entry in PPCM-treated HeLa cells. MLV pGag-Pol plasmid (packaging plasmid), pZaire Ebola Glycoprotein plasmid (envelope plasmid), and pmStrawberry reporter gene plasmid (Transfer plasmid) were kindly provided by Dr. Robert A. Davey (Boston University, Boston, USA). Briefly, the 3 plasmids were mixed and transfected into 293T cells for 10 h using Mirus-LT1 classic transfection protocol. The medium was then discarded and replaced by fresh DMEM 1% FBS. At 48 h post-transfection, the culture supernatant containing MLV-Ebola was collected, clarified by centrifugation at 220*g* for 10 min and filtration (0.45 µm pore-size), and then used in transduction assays in HeLa and VK2/E6E7 cells. All experiments using the replication-defective MLV-Ebola were performed under biosafety level 2 (BSL2) containment.

To determine the level of transduction, 3 × 10^5 cells were plated the day before infection in a 12-well plate format. One hour prior to infection, cell medium was replaced by 1 ml of fresh DMEM 1% FBS or full Keratinocyte-Serum Free medium containing PPCM when appropriate. Medium was then removed, with no PBS rinse, and cells were incubated with the clarified culture supernatant containing MLV-EBOV for 36 h. The percentage of Strawberry-positive cells was determined on a LSRFortessa flow cytometer (BD Biosciences), following individualization of cells and fixation in 4% formaldehyde in PBS. The percentage of transduced cells in MLV-EBOV-infected cells without PPCM treatment was compared to the reciprocals in PPCM-pretreated cells. Control of complete inhibition was done by pre-incubation of MLV-EBOV with the neutralizing monoclonal S9 antibody for 1 h prior to infection.

2.9. Bio-plex assay

Cytokine and chemokine concentrations in cell-free supernatants of VK2/E6E7 were determined using a combination of Bio-Plex Pro Human inflammation panel 1 37-plex and cytokine group 1 panel 27-plex Immunoassay kits (Bio-Rad). The concentration of 59 analytes (Chitinase-3-like, Eotaxin, FGF-basic, G-CSF, GM-CSF, IL-1Rα, IL-1β, IL-2, IL-4, IL-5, IL-6, sIL-6Rα, sIL-6Rβ, IL-7, IL-8, IL-9, IL-10, IL-11, IL-12 (p40), IL-12 (p70), IL-13, IL-15, IL-17, IL-19, IL-20, IL-22, IL-26, IL-27, IL-32, IL-34, IL-35, IFN-α2, IFN-β, IFN-γ, IFN-λ1, IFN-λ2, IP-10, MMP-1, MMP-2, MMP-3, MCP-1, MIP-1α, MIP-1β, Osteocalcin, Osteopontin, Pentraxin-3, RANTES, sCD163, TNF-α, sTNF-R1, sTNF-R2, TNFRSF8, TNFSF12, TNFSF13, TNFSF13B, TNFSF14, TSLP, PDGF-BB, and VEGF) were quantified. Samples from EBOV-infected cells were inactivated on dry ice by gamma irradiation (5 Mrad) prior to removal from the BSL4 laboratory following approved standard operating protocols for analysis at BSL2.

2.10. Statistical analysis

One-way analysis of variance (ANOVA) with Tukey's post-hoc analysis was used in multiple comparisons. Null hypotheses were rejected at *P* values less than 0.05. All data presented in figures represent means ± standard error (*p < 0.05, **p < 0.01, ***p < 0.001). Virus kinetic experiments, transduction assays, and inflammatory response multiplex assays were performed with biological triplicates. Biological duplicates or triplicates were used in EBOV GP-cell binding assays depending on the cell type. Automated cell counting was performed based on 3 fields of view per experimental condition. Statistical analysis was performed with GraphPad Prism 5 software (GraphPad Software, Inc.).

3. Results

3.1. Polyphenylene carboxymethylene (PPCM) interferes with EBOV replication

Virus infection kinetics were initially performed on the permissive Vero cell line and then repeated, as a proof of concept, on HeLa and VK2/E6E7 cells from the human cervical or vaginal epithelium to investigate their respective susceptibility to infection as well as to assess the potential antiviral activity of PPCM against EBOV in the context of a sexually transmitted disease. The Cytotoxic Concentration (CC_{50}) of PPCM for each cell type was determined prior virus replication kinetics, and was consistent with dose ranges at which PPCM was previously used in macrophages, dendritic cells, and lymphocytes to demonstrate microbial effect (Chang et al., 2007; Herold et al., 2002). Specifically, CC_{50} was here above 3 mg/ml, 30 µg/ml, and 0.9 mg/ml for Vero, HeLa, or VK2/E6E7 cells (Supplementary Fig. 1), respectively, when cultured for 5 additional days after plating. This is typically an incubation time sufficient for EBOV-eGFP to reach high titers in Vero cells (Bazhanov et al., 2017).

PPCM treatment significantly decreased virus replication in Vero cells in a dose-dependent manner ranging from 2 mg/ml to 10 µg/ml, irrespective of the multiplicity of infection (MOI) (Fig. 1A and B). Specifically, 2 mg/ml PPCM treatment lowered virus titer at day 5 post-infection (pi) by more than 1 and 2 $\log_{10}$, when added respectively after 1 h post-infection (no pre-treatment) or 1 h prior infection (pre-treatment), and then again 1 h after infection using a high MOI (Fig. 1A). When infecting cells with a 100-fold lower MOI, any concentration above 1 mg/ml lowered virus titer by more than 3 $\log_{10}$ or was under the limit of detection (Fig. 1B). All these effects were similarly observed

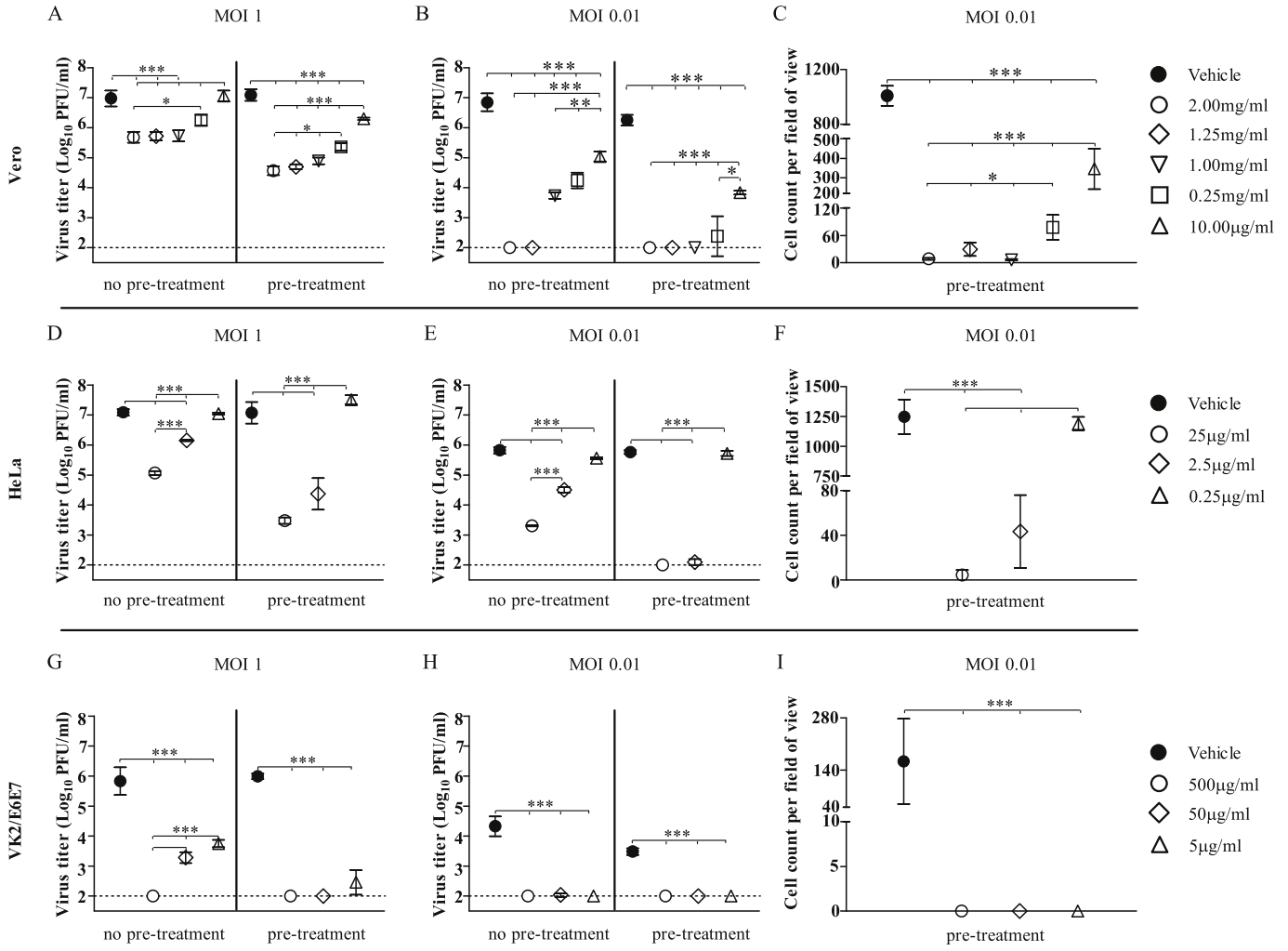

Fig. 1. Polyphenylene carboxymethylene (PPCM) interferes with EBOV replication. EBOV replication in **(A–C)** Vero, **(D–F)** HeLa, and **(G–I)** VK2/E6E7 cells at day 5 post-infection. Assay performed using a high and low multiplicity of infection (MOI) with PPCM treatments starting either 1 h post-infection (no pre-treatment) or 1 h prior infection (pre-treatment). The horizontal dotted line corresponds to the detection limit. Automated counting of infected **(C)** Vero, **(F)** HeLa, or **(I)** VK2/E6E7 cells per field of view under 10× magnification using CellProfiler. Results are expressed as the average of 3 repetitions; error bars represent standard deviations. *, $P < 0.05$ **, $P < 0.01$; ***, $P < 0.001$ (ANOVA-Tukey's multiple-comparison test).

by day 3 pi (data not shown). Therefore, the highest antiviral efficacy was achieved when PPCM treatment started prior to infection suggesting a direct interaction of PPCM with cells. Further analysis of virus replication using a low MOI revealed that although virus titer was under the sensitivity of our assay with the 3 highest concentrations tested, an average of 4–55 cells remained infected per field of view (Fig. 1C) suggesting that infected cells can still be identified. The antiviral activity of PPCM was also dose-dependent in HeLa (Fig. 1D–F) and VK2/E6E7 (Fig. 1G–I) cells, from respectively 25 µg/ml to 2.5 µg/ml or from 500 µg/ml to at least 5 µg/ml, at day 5 post-infection. The highest PPCM dose lowered virus titer by at least 2 or 4 $\log_{10}$, when treatment started 1 h prior infection (pre-treatment), using a high MOI in both cell types (Fig. 1D, G). However, the highest antiviral effect was reached against a low MOI when HeLa and VK2/E6E7 cells were pretreated for 1 h prior infection (pre-treatment) with the highest or any PPCM dose, respectively (Fig. 1E, H). Although, an average of 5 cells per field of view were still positive for eGFP expression in HeLa cells pretreated with the highest PPCM dose (Fig. 1F), none could be found using VK2/E6E7 cells irrespective of PPCM dose (Fig. 1I). It is interesting to note that virus replication using a low MOI was significantly delayed in VK2/E6E7 compared to Vero cells at day 3 (data not shown) and 5 post-infection (Fig. 1B, and H) suggesting a lower susceptibility of vaginal epithelial cells for the virus, which increased as a result the antiviral effect of PPCM in a 5 day time frame of infection.

Because PPCM is intended to be applied prior intercourse, and normal vaginal epithelial cells infected by a low MOI are likely relevant to mimic a natural infection originating from a survivor long after onset of disease, we further investigated gene expression of the EBOV glycoprotein (GP) in these specific VK2/E6E7 samples. Assessment of EBOV and 18sRNA gene expression in mock-infected PPCM pretreated VK2/E6E7 cells was used to determine the cut-off (ΔCt) for positive samples (Table 1) and showed that virus genome in EBOV-infected VK2/E6E7 cells was either at the limit of detection or undetectable (Table 1). However, subsequent passage on Vero cells of culture supernatants from any of these PPCM pretreated VK2/E6E7 cells failed to retrieve infectious virus except for one replicate incubated with the lowest PPCM concentration resulting in a virus titer of 4.0×10^2 pfu/ml (Table 2). No virus genome was detected in Vero cells as well, except for 2 out of 3 of the aforementioned replicates (Table 2). These data suggest that PPCM can abolish EBOV replication in the vaginal epithelium.

3.2. PPCM interference with EBOV cell attachment

A soluble truncated form of the EBOV GP was used as a surrogate of the infectious virus in a GP-Vero, -HeLa, and -VK2/E6E7 binding assay

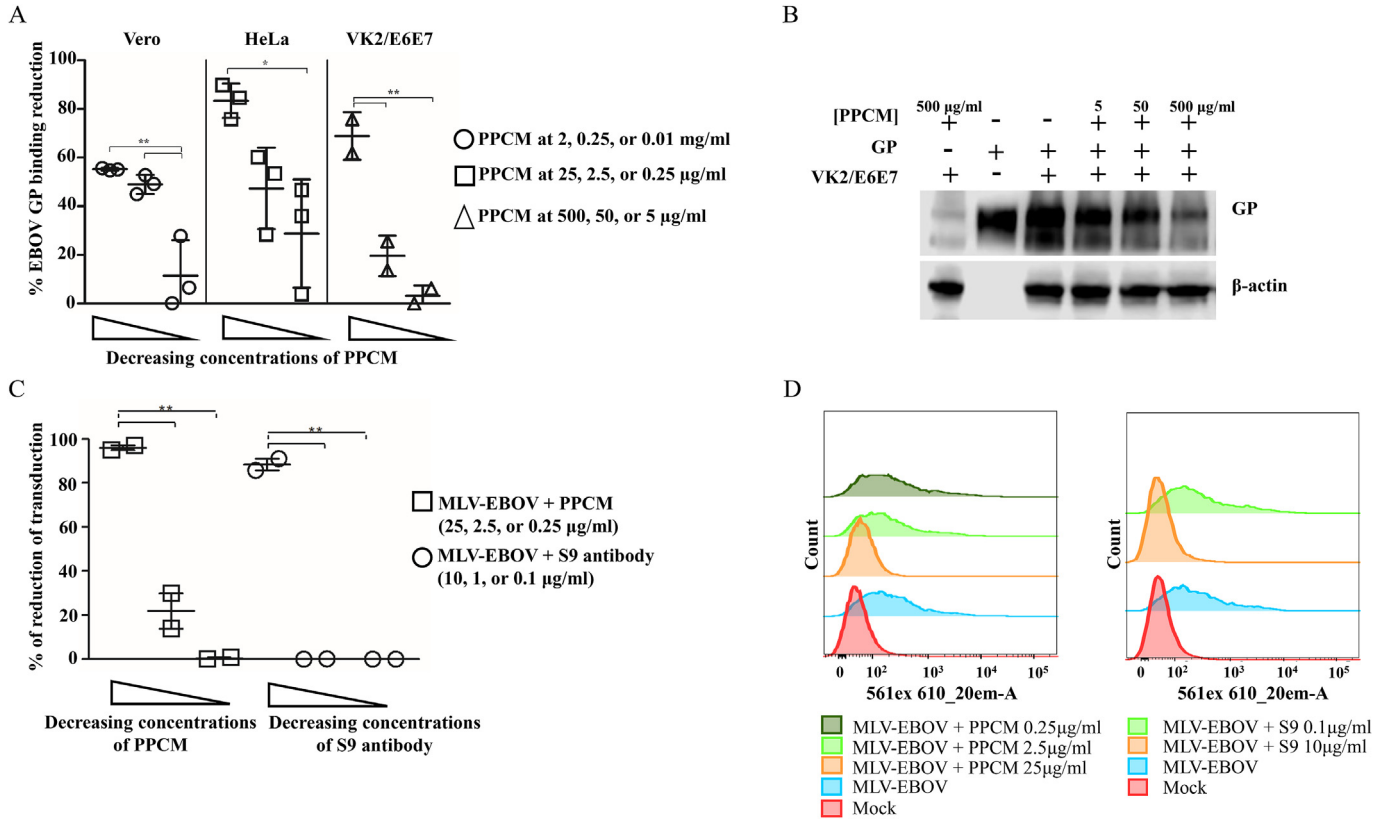

Fig. 2. PPCM interference with EBOV cell attachment and EBOV replication cycle. PPCM reduction of EBOV GP-cell binding is dose-dependent **(A, B)** and PPCM interferes with MLV-Ebola early on the replication cycle **(C, D)**.. **(A)** Percentage reduction of EBOV-GP bound to Vero, HeLa, or VK2/E6E7 when GP is preliminary incubated with decreasing concentrations of PPCM. **(B)** Detection of EBOV-GP_1 by SDS-PAGE illustrating typical changes in GP binding efficacy to VK2/E6E7 cells when GP is preincubated with increasing concentrations of PPCM. **(C)** Percentage reduction of MLV-EBOV transduction in PPCM-pretreated compared to untreated HeLa cells. Results are expressed as the average of at least 2 biological replicates; error bars represent standard deviations. *, $P < 0.05$ **, $P < 0.01$ (ANOVA-Tukey's multiple-comparison test). **(D)** One-parameter histograms plotting strawberry fluorescence signal intensity versus number of cells. Typical transduction levels of MLV-EBOV in HeLa cells preincubated with different concentrations of PPCM (left side). Control of complete inhibition of transduction was done by incubating MLV-EBOV with the neutralizing Mab S9 prior inoculation to cells (right side).

to evaluate whether PPCM interferes with EBOV replication, and notably the direct effect of PPCM on virus particles. The amount of GP recovered without any PPCM treatments was compared to the amount of GP recovered after cells were pre-incubated with variable doses of PPCM. The amount of GP bound to either of the three cell types was PPCM dose-dependent (Fig. 2A and B). Indeed, a PPCM solution at 2, 0.25, and 0.01 mg/ml reduced respectively by 55, 48, and 11% the amount of GP bound to Vero cells. Likewise, a PPCM solution at 25, 2.5, and 0.25 µg/ml reduced respectively by 82, 47, and 28% the amount of GP bound to HeLa cells. Finally, a reduction in GP binding to VK2/E6E7 cells was 48, 19, and 3%, respectively, when using PPCM at 500, 50, and 5 µg/ml (Fig. 2B). These data suggest that PPCM interferes with GP in the viral attachment process to cells.

3.3. PPCM antiviral activity on EBOV life cycle

Next, we explored which early steps of the virus life cycle might be affected by PPCM in addition to interfering with attachment of EBOV to host cells. As PPCM does not enter the cells due to its physicochemical properties including a large molecular weight, we explored a possible interference at the virus entry step using a replication-defective recombinant murine leukemia virus pseudotyped with EBOV GP (MLV-EBOV) and carrying the fluorescent Strawberry transgene. MLV-EBOV transduced on average 7% of VK2/E6E7 cells (data not shown), and on average 25% of HeLa cells (Fig. 2C and D). Considering the antiviral effect of PPCM against EBOV in HeLa and VK2/E6E7 cells and as a proof of concept, virus transduction efficacy was further conducted with the former cells only. However, 25 µg/ml PPCM 1 h pre-treatment prior to infection resulted in complete (100%) inhibition of transduction. These data are similar to the positive control incubation of MLV-EBOV with the neutralizing monoclonal S9 antibody (Hernandez et al., 2015; Marceau et al., 2014) (Fig. 2C and D). Consistent with virus replication kinetics and EBOV GP-cell binding data, there was a dose-dependent inhibition of MLV-EBOV transduction since a 2.5 and 0.25 µg/ml PPCM dose only reduced it respectively by 40% and 10%, compared to untreated cells. These data suggest that PPCM interferes at least in part at the virus entry step of EBOV replication cycle.

3.4. Inflammatory response of human normal vaginal epithelial cells following EBOV infection

An exacerbated inflammatory response is a key feature of EVD. No published data are available describing this response in EBOV-infected normal cells of the human reproductive system. The inflammatory response of EBOV-infected VK2/E6E7 cells using both a high and low infective dose was investigated at day 5 post-infection. EBOV infection in our study resulted in a significantly increased secretion of at least 5 chemokines (Eotaxin, IL-8, IP-10, MIP-1β, and RANTES) and 10 cytokines/soluble cytokine receptors (IFN-β, IFN-γ, IFN-λ1, IFN-λ2, sIL 6-Rα, IL-6, IL-7, IL-9, IL-11, and TNF-α) when a high infective dose was used (Fig. 3). However, the amount of IFN-γ, IFN-λ2, IL-6, IL-7, IL-8, IL-9, IP-10, and MIP-1β were not-significantly different between mock- and EBOV-infected cells using a low infective dose (data not shown), suggesting that inflammatory response was partially delayed, possibly

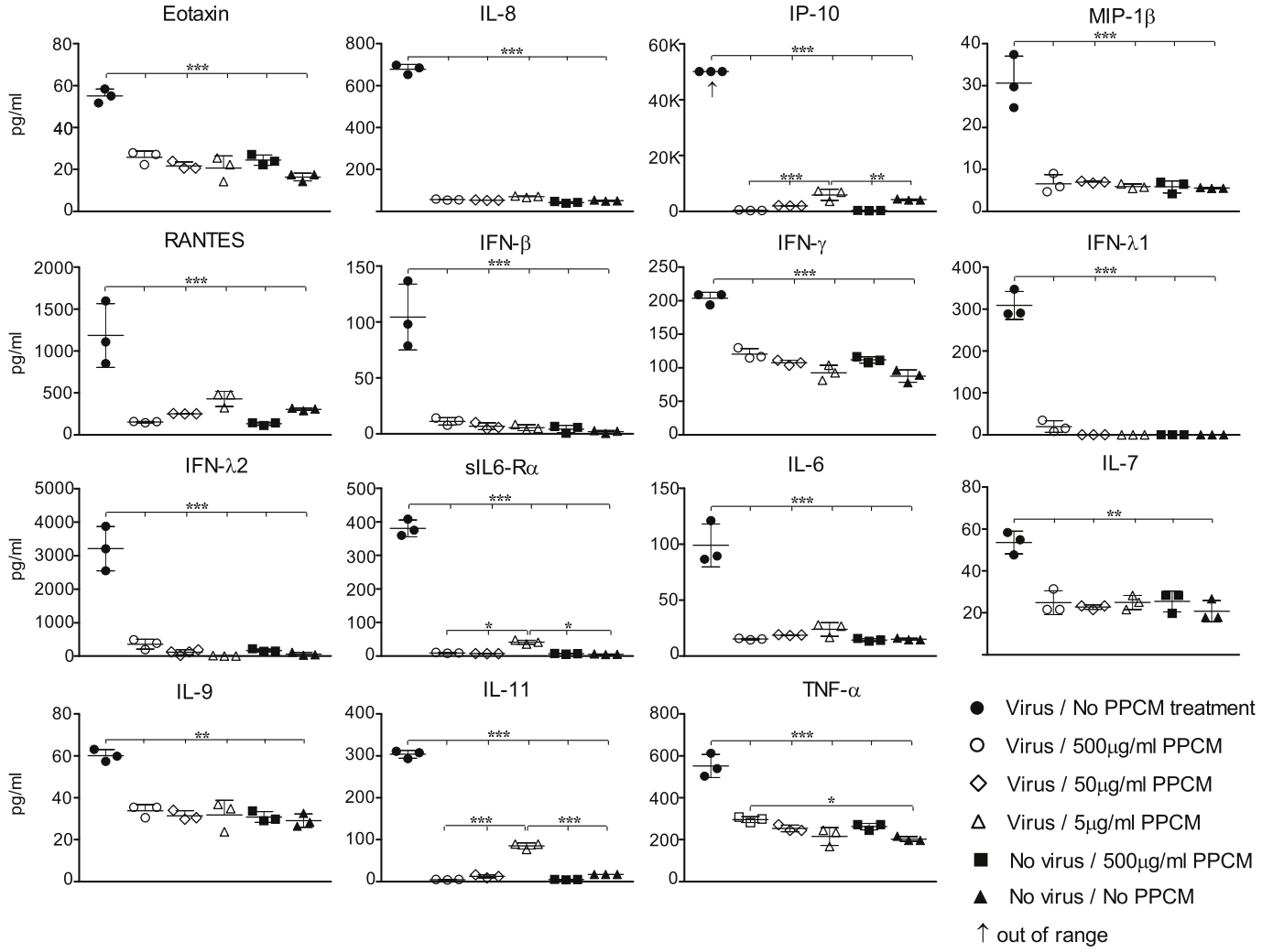

Fig. 3. Inflammatory response of human normal vaginal epithelial cells (VK2/E6E7) following EBOV infection, and effect of PPCM. Shown are cytokine/chemokine levels in EBOV-infected cells using a MOI of 1, with or without PPCM treatment post-infection, compared to mock-infected cells at day 5 post-infection. Results are expressed as averages of data from biological triplicates, and bars represent standard deviations. **, $P < 0.01$; ***, $P < 0.001$ (ANOVA-Tukey's multiple-comparison test).

due to lower levels of replication detected at that same time (Fig. 1).

When introducing PPCM treatments and using a high MOI in order to synchronize the infection, the anti-inflammatory effect was similar whether cells started being treated with PPCM after (no pre-treatment) or prior (pre-treatment) to infection (Fig. 3; Supplementary Fig. 2). Interestingly, the secretion levels of the 5 chemokines and 10 cytokines above were comparable between EBOV-infected cells treated with 500 or 50 μg/ml PPCM, mock-infected cells treated with 500 μg/ml PPCM, and mock-infected cells (Fig. 3). However, the anti-inflammatory effect of PPCM was dose-dependent as shown by increasing secretions of sIL-6Rα, IL-6, IL-8, IL-11, IP-10, and of RANTES when PPCM dose was decreased to 5 μg/ml (Fig. 3). This was consistent with higher virus replication levels compared to the counterparts when a 500 or 50 μg/ml PPCM dose was used (Fig. 1). These data suggest that PPCM does not cause any inflammatory response at the highest dose tested in vaginal epithelial cells, and that it can maintain a level of inflammation comparable to mock-infected cells even though virus is replicating.

4. Discussion

Male-to-female sexual transmission of a filovirus was first documented during the 1967 Marburg virus disease outbreak in Germany (Martini and Schmidt, 1968; Slenczka and Klenk, 2007). Later, studies reported that Ebola virus genome and infectious virus was isolated from the semen of convalescent patients during the 1995 and 2000 outbreak (Rodriguez et al., 1999; Rowe et al., 1999), and abstinence was then recommended for at least 3 months after recovery to avoid a possible secondary transmission. However, sexual transmission of Ebola virus through survivors was demonstrated later during the 2014–2016 outbreak in West Africa (Mate et al., 2015).

Currently, no published data are available regarding the efficacy of antimicrobial products against EBOV in the context of a sexually transmitted infection (STI). In this study, we demonstrated the interference of PPCM with a low infective dose of EBOV in normal vaginal epithelial cells, as shown by undetectable virus titer (lower than 100 pfu/ml), low to no virus genome, and no virus replication-related eGFP expression. Although a low infective dose likely mimics a natural infection transmitted from an EBOV survivor long after onset of disease it is interesting to note that direct virus replication in semen of one patient was reported until at least 110 days after onset of disease (Barnes et al., 2017). This may increase persistence and long-term transmission efficacy and will require further investigations. Even though EBOV infective dose is thought to be low (Bausch et al., 2007), inoculation of fresh Vero cells with day 5 culture supernatants from originally infected 500 or 50 μg/ml PPCM pre-treated VK2/E6E7 failed to retrieve any infectious virus or virus genome, suggesting that PPCM

can neutralize a low dose of EBOV on the vaginal mucosa. These data are also in line with the antiviral effect of PPCM described for HIV and HSV at similar doses (Herold et al., 2002).

PPCM directly interacts with EBOV glycoprotein (GP) suggesting a possible interference with its glycan cap binding to C-Type Lectin cell receptors (CLRs) (Alvarez et al., 2002; Simmons et al., 2003) used by EBOV for non-specific cell attachment to cells (Emanuel et al., 2018; Moller-Tank and Maury, 2015). EBOV GP attachment is mediated by the N- and O-glycans clustered on the mucin-like domain of the GP_1 subunit but identification of the type of interaction with the negatively charged PPCM polymer will require further investigations. Interestingly, pre-treatment of cells also significantly increased PPCM antiviral effect suggesting that the activity is also related to direct contact with cells and is consistent with PPCM blocking virus entry of the replication-defective MLV-EBOV GP in PPCM-pretreated cells. PPCM has broad-spectrum antiviral properties and was previously shown to interfere with the envelope glycoprotein 120 of HIV and B of HSV in the cell attachment process (Herold et al., 2002). It is unclear which domain of these glycoproteins interacts with PPCM; however, the authors suggest that PPCM is competing for the ubiquitous cell surface glycosaminoglycan heparan sulfate (HS) which mediates HIV infectivity efficiency (Mondor et al., 1998; Ohshiro et al., 1996), and also constitutes the primary attachment receptor for HSV (Shieh et al., 1992). Interestingly, the importance of HS in facilitating infection is documented among viruses from multiple families (Chen et al., 1997; de Boer et al., 2012; Klimyte et al., 2016; Kroschewski et al., 2003; O'Hearn et al., 2015), including Ebola virus (O'Hearn et al., 2015; Salvador et al., 2013). A recent study highlighted the importance of HS in EBOV infection of epithelial cells, as enzymatic cleavage of HS reduced virus binding and inhibited infection (Tamhankar et al., 2018). Altogether, this suggests that PPCM antiviral activity against EBOV occurs at the early steps of infection and is likely mediated by PPCM both neutralizing GP binding to cells and competing with EBOV for HS binding on cells. However, it is unknown whether PPCM also inhibits infection through blockage of EBOV attachment to phosphatidylserine cell receptors (Moller-Tank and Maury, 2015), as well as if it affects expression of the GP-dependent cell surface macropinocytosis inducers (Nanbo et al., 2010) required for virus entry by macropinocytosis (Aleksandrowicz et al., 2011; Nanbo et al., 2010; Saeed et al., 2010).

Characterization of inflammation in response to infection was done from cells infected at a high MOI in order to have a synchronized response. Vaginal epithelial cells play an important role in the innate immune response to EBOV in the context of a STI as they are at the interface of infection and demonstrated permissiveness to virus replication in our study. This is consistent with the secretion of type I, II, and III interferon (IFN), which constitutes a complex anti-viral response initiated by sensing both EBOV genome inside the cell cytoplasm and EBOV particles at the cell membrane through pathogen recognition receptors (PRRs) (Ayithan et al., 2014; Olejnik et al., 2017). Mechanistically, this results in activation of IFN JAK-STAT pathways leading to transcriptional expression of antiviral interferon-stimulated genes to counteract the infection (Pinto et al., 2015; Rhein et al., 2015). Interestingly, secretion of type III IFN, here λ1 and λ2, has not been reported during EBOV infection, suggesting that it is a cell-specific response. Induction of type III IFN is mediated by PRRs that are either Ku70, Toll-like, or RIG-I-like receptors (Ank et al., 2008; Chandra et al., 2014; Odendall et al., 2014; Stoltz and Klingstrom, 2010; Zhang et al., 2011). As Ku70 is a DNA sensor, only the two latter are relevant to EBOV. Therefore, type III IFN expression might be due to sensing of EBOV particles by different Toll-like receptors (TLRs) than the previously described TLR4 (Ayithan et al., 2014) or by TLR4 with other downstream signaling factors than IRF3/IRF7 that would otherwise induce type I IFN. Alternatively, this could be induced by sensing EBOV genome through the RIG-I-like–MAVS pathway with proteins, including IRF1, that selectively control type III IFN expression (Odendall et al., 2014), but this will require further investigations. Presence of IFN was also accompanied of overly secreted proinflammatory mediators such as IL-6, IL-8, IP-10, MIP-1β, RANTES, and TNF-α as a result of the NF-κB pathway activation (Martinez et al., 2007), suggesting inflammation of the vaginal epithelium. Interestingly, while immune response in mock-infected cells was comparable to the reciprocal in either of the EBOV-infected 500 or 50 μg/ml PPCM pre-treated VK2/E6E7 cells, virus replication was still detectable in the latter. This could be explained by a suboptimal concentration of PPCM that is inhibiting or delaying PRRs activation.

In conclusion, our study investigated the *in vitro* antiviral efficacy of PPCM against EBOV infection in the context of a sexually transmitted disease. We demonstrated the permissiveness of EBOV infection in normal vaginal epithelial cells and reported an atypical innate immune response to EBOV through secretion of IFN λ. We also showed that PPCM inhibited EBOV infection by directly interfering with EBOV GP and by likely masking cell attachment receptors such as HS. Our data support the importance of studying this route of infection and its role in the multiple flare-ups during the largest ever-documented 2014–2016 EBOV outbreak in West Africa. This study also supports that PPCM should be evaluated *in vivo* as a potential topical microbicide effective against EBOV, and potentially other filoviruses.

Declarations of interest

None.

Acknowledgements and Funding

We thank Yaso Therapeutics Inc. (supported by NIH R42AI069659, R43/44 084225 and R44092206) for generously providing VK2/E6E7 cells with the corresponding culture reagents, and PPCM master stock. This work was partially supported by NIH grant R33AI102267 (A.N.F.).

Appendix A. Supplementary data

Supplementary data to this article can be found online at https://doi.org/10.1016/j.antiviral.2019.104567.

References

Aleksandrowicz, P., Marzi, A., Biedenkopf, N., Beimforde, N., Becker, S., Hoenen, T., Feldmann, H., Schnittler, H.J., 2011. Ebola virus enters host cells by macropinocytosis and clathrin-mediated endocytosis. J. Infect. Dis. 204 (Suppl. 3), S957–S967.

Alvarez, C.P., Lasala, F., Carrillo, J., Muniz, O., Corbi, A.L., Delgado, R., 2002. C-type lectins DC-SIGN and L-SIGN mediate cellular entry by Ebola virus in cis and in trans. J. Virol. 76, 6841–6844.

Ank, N., Iversen, M.B., Bartholdy, C., Staeheli, P., Hartmann, R., Jensen, U.B., Dagnaes-Hansen, F., Thomsen, A.R., Chen, Z., Haugen, H., Klucher, K., Paludan, S.R., 2008. An important role for type III interferon (IFN-lambda/IL-28) in TLR-induced antiviral activity. J. Immunol. 180, 2474–2485.

Ayithan, N., Bradfute, S.B., Anthony, S.M., Stuthman, K.S., Dye, J.M., Bavari, S., Bray, M., Ozato, K., 2014. Ebola virus-like particles stimulate type I interferons and proinflammatory cytokine expression through the toll-like receptor and interferon signaling pathways. J. Interferon Cytokine Res. : Off. J. Int. Soc. Inter. Cytokine Res. 34, 79–89.

Barnes, K.G., Kindrachuk, J., Lin, A.E., Wohl, S., Qu, J., Tostenson, S.D., Dorman, W.R., Busby, M., Siddle, K.J., Luo, C.Y., Matranga, C.B., Davey, R.T., Sabeti, P.C., Chertow, D.S., 2017. Evidence of ebola virus replication and high concentration in semen of a patient during recovery. Clin. Infect. Dis. : Off. Publ. Infect. Dis. Soc. Am. 65, 1400–1403.

Bausch, D.G., Towner, J.S., Dowell, S.F., Kaducu, F., Lukwiya, M., Sanchez, A., Nichol, S.T., Ksiazek, T.G., Rollin, P.E., 2007. Assessment of the risk of Ebola virus transmission from bodily fluids and fomites. J. Infect. Dis. 196 (Suppl. 2), S142–S147.

Bazhanov, N., Escaffre, O., Freiberg, A.N., Garofalo, R.P., Casola, A., 2017. Broad-range antiviral activity of hydrogen sulfide against highly pathogenic RNA viruses. Sci. Rep. 7, 41029.

Carpenter, A.E., Jones, T.R., Lamprecht, M.R., Clarke, C., Kang, I.H., Friman, O., Guertin, D.A., Chang, J.H., Lindquist, R.A., Moffat, J., Golland, P., Sabatini, D.M., 2006. CellProfiler: image analysis software for identifying and quantifying cell phenotypes. Genome Biol. 7, R100.

Chandra, P.K., Bao, L., Song, K., Aboulnasr, F.M., Baker, D.P., Shores, N., Wimley, W.C., Liu, S., Hagedorn, C.H., Fuchs, S.Y., Wu, T., Balart, L.A., Dash, S., 2014. HCV

infection selectively impairs type I but not type III IFN signaling. Am. J. Pathol. 184, 214–229.
Chang, T.L., Teleshova, N., Rapista, A., Paluch, M., Anderson, R.A., Waller, D.P., Zaneveld, L.J., Granelli-Piperno, A., Klotman, M.E., 2007. SAMMA, a mandelic acid condensation polymer, inhibits dendritic cell-mediated HIV transmission. FEBS Lett. 581, 4596–4602.
Chen, Y., Maguire, T., Hileman, R.E., Fromm, J.R., Esko, J.D., Linhardt, R.J., Marks, R.M., 1997. Dengue virus infectivity depends on envelope protein binding to target cell heparan sulfate. Nat. Med. 3, 866–871.
Christie, A., Davies-Wayne, G.J., Cordier-Lassalle, T., Blackley, D.J., Laney, A.S., Williams, D.E., Shinde, S.A., Badio, M., Lo, T., Mate, S.E., Ladner, J.T., Wiley, M.R., Kugelman, J.R., Palacios, G., Holbrook, M.R., Janosko, K.B., de Wit, E., van Doremalen, N., Munster, V.J., Pettitt, J., Schoepp, R.J., Verhenne, L., Evlampidou, I., Kollie, K.K., Sieh, S.B., Gasasira, A., Bolay, F., Kateh, F.N., Nyenswah, T.G., De Cock, K.M., Centers for Disease, C., Prevention, 2015. Possible sexual transmission of Ebola virus - Liberia, 2015. MMWR. Morb. Mort. Weekly Rep. 64, 479–481.
Commission, R.o.a.I., 1978. Ebola haemorrhagic fever in Zaire, 1976. Bull. World Health Organ. 56, 271–293.
Crozier, I., 2016. Ebola virus RNA in the semen of male survivors of ebola virus disease: the uncertain gravitas of a privileged persistence. J. Infect. Dis. 214, 1467–1469.
de Boer, S.M., Kortekaas, J., de Haan, C.A., Rottier, P.J., Moormann, R.J., Bosch, B.J., 2012. Heparan sulfate facilitates Rift Valley fever virus entry into the cell. J. Virol. 86, 13767–13771.
Deen, G.F., Broutet, N., Xu, W., Knust, B., Sesay, F.R., McDonald, S.L.R., Ervin, E., Marrinan, J.E., Gaillard, P., Habib, N., Liu, H., Liu, W., Thorson, A.E., Yamba, F., Massaquoi, T.A., James, F., Ariyarajah, A., Ross, C., Bernstein, K., Coursier, A., Klena, J., Carino, M., Wurie, A.H., Zhang, Y., Dumbuya, M.S., Abad, N., Idriss, B., Wi, T., Bennett, S.D., Davies, T., Ebrahim, F.K., Meites, E., Naidoo, D., Smith, S.J., Ongpin, P., Malik, T., Banerjee, A., Erickson, B.R., Liu, Y., Liu, Y., Xu, K., Brault, A., Durski, K.N., Winter, J., Sealy, T., Nichol, S.T., Lamunu, M., Bangura, J., Landoulsi, S., Jambai, A., Morgan, O., Wu, G., Liang, M., Su, Q., Lan, Y., Hao, Y., Formenty, P., Stroher, U., Sahr, F., 2017. Ebola RNA persistence in semen of ebola virus disease survivors - final report. N. Engl. J. Med. 377, 1428–1437.
Dhama, K., Karthik, K., Khandia, R., Chakraborty, S., Munjal, A., Latheef, S.K., Kumar, D., Ramakrishnan, M.A., Malik, Y.S., Singh, R., Malik, S.V.S., Singh, R.K., Chaicumpa, W., 2018. Advances in designing and developing vaccines, drugs, and therapies to counter ebola virus. Front. Immunol. 9, 1803.
Emanuel, J., Marzi, A., Feldmann, H., 2018. Filoviruses: ecology, molecular biology, and evolution. Adv. Virus Res. 100, 189–221.
Emond, R.T., Evans, B., Bowen, E.T., Lloyd, G., 1977. A case of Ebola virus infection. Br. Med. J. 2, 541–544.
Etard, J.F., Sow, M.S., Leroy, S., Toure, A., Taverne, B., Keita, A.K., Msellati, P., Magassouba, N., Baize, S., Raoul, H., Izard, S., Kpamou, C., March, L., Savane, I., Barry, M., Delaporte, E., Postebogui Study, G., 2017. Multidisciplinary assessment of post-Ebola sequelae in Guinea (Postebogui): an observational cohort study. Lancet Infect. Dis. 17, 545–552.
Feldmann, H., Geisbert, T.W., 2011. Ebola haemorrhagic fever. Lancet 377, 849–862.
Feldmann, H., Sanchez, A., Geisbert, T.W., 2013. Filoviridae: marburg and ebola viruses. In: sixth ed. Fields Virology, vol 1 Wolters Kluwer Health Adis (ESP).
Fischer, W.A., Brown, J., Wohl, D.A., Loftis, A.J., Tozay, S., Reeves, E., Pewu, K., Gorvego, G., Quellie, S., Cunningham, C.K., Merenbloom, C., Napravnik, S., Dube, K., Adjasoo, D., Jones, E., Bonarwolo, K., Hoover, D., 2017. Ebola virus ribonucleic acid detection in semen more than two years after resolution of acute ebola virus infection. Open Forum Infect. Dis. 4 ofx155.
Henao-Restrepo, A.M., Camacho, A., Longini, I.M., Watson, C.H., Edmunds, W.J., Egger, M., Carroll, M.W., Dean, N.E., Diatta, I., Doumbia, M., Draguez, B., Duraffour, S., Enwere, G., Grais, R., Gunther, S., Gsell, P.S., Hossmann, S., Watle, S.V., Konde, M.K., Keita, S., Kone, S., Kuisma, E., Levine, M.M., Mandal, S., Mauget, T., Norheim, G., Riveros, X., Soumah, A., Trelle, S., Vicari, A.S., Rottingen, J.A., Kieny, M.P., 2017. Efficacy and effectiveness of an rVSV-vectored vaccine in preventing Ebola virus disease: final results from the Guinea ring vaccination, open-label, cluster-randomised trial (Ebola Ca Suffit!). Lancet 389, 505–518.
Henao-Restrepo, A.M., Longini, I.M., Egger, M., Dean, N.E., Edmunds, W.J., Camacho, A., Carroll, M.W., Doumbia, M., Draguez, B., Duraffour, S., Enwere, G., Grais, R., Gunther, S., Hossmann, S., Konde, M.K., Kone, S., Kuisma, E., Levine, M.M., Mandal, S., Norheim, G., Riveros, X., Soumah, A., Trelle, S., Vicari, A.S., Watson, C.H., Keita, S., Kieny, M.P., Rottingen, J.A., 2015. Efficacy and effectiveness of an rVSV-vectored vaccine expressing Ebola surface glycoprotein: interim results from the Guinea ring vaccination cluster-randomised trial. Lancet 386, 857–866.
Hernandez, H., Marceau, C., Halliday, H., Callison, J., Borisevich, V., Escaffre, O., Creech, J., Feldmann, H., Rockx, B., 2015. Development and characterization of broadly cross-reactive monoclonal antibodies against all known Ebolavirus species. J. Infect. Dis. 212 (Suppl. 2), S410–S413.
Herold, B.C., Scordi-Bello, I., Cheshenko, N., Marcellino, D., Dzuzelewski, M., Francois, F., Morin, R., Casullo, V.M., Anderson, R.A., Chany 2nd, C., Waller, D.P., Zaneveld, L.J., Klotman, M.E., 2002. Mandelic acid condensation polymer: novel candidate microbicide for prevention of human immunodeficiency virus and herpes simplex virus entry. J. Virol. 76, 11236–11244.
Keita, A.K., Toure, A., Sow, M.S., Raoul, H., Magassouba, N., Delaporte, E., Etard, J.F., Group, P.S., 2017. Extraordinary long-term and fluctuating persistence of Ebola virus RNA in semen of survivors in Guinea: implications for public health. Clin. Microbiol. Infect. : Off. Publ. Eur. Soc. Clin. Microbiol. Infect. Dis. 23, 412–413.
Klimyte, E.M., Smith, S.E., Oreste, P., Lembo, D., Dutch, R.E., 2016. Inhibition of human metapneumovirus binding to heparan sulfate blocks infection in human lung cells and airway tissues. J. Virol. 90, 9237–9250.
Kroschewski, H., Allison, S.L., Heinz, F.X., Mandl, C.W., 2003. Role of heparan sulfate for attachment and entry of tick-borne encephalitis virus. Virology 308, 92–100.
Lamprecht, M.R., Sabatini, D.M., Carpenter, A.E., 2007. CellProfiler: free, versatile software for automated biological image analysis. Biotechniques 42, 71–75.
Luo, D., Zheng, R., Wang, D., Zhang, X., Yin, Y., Wang, K., Wang, W., 2019. Effect of sexual transmission on the West Africa Ebola outbreak in 2014: a mathematical modelling study. Sci. Rep. 9, 1653.
Madelain, V., Nguyen, T.H., Olivo, A., de Lamballerie, X., Guedj, J., Taburet, A.M., Mentre, F., 2016. Ebola virus infection: review of the pharmacokinetic and pharmacodynamic properties of drugs considered for testing in human efficacy trials. Clin. Pharmacokinet. 55, 907–923.
Marceau, C.D., Negi, S.S., Hernandez, H., Callison, J., Marzi, A., Borisevich, V., Braun, W., Berry, J., Feldmann, H., Rockx, B., 2014. Novel neutralizing monoclonal antibodies protect rodents against lethal filovirus challenges. Trials Vaccinol. 3, 89–94.
Martinez, O., Valmas, C., Basler, C.F., 2007. Ebola virus-like particle-induced activation of NF-kappaB and Erk signaling in human dendritic cells requires the glycoprotein mucin domain. Virology 364, 342–354.
Martini, G.A., Schmidt, H.A., 1968. [Spermatogenic transmission of the "Marburg virus". (Causes of "Marburg simian disease")]. Klin. Wochenschr. 46, 398–400.
Mate, S.E., Kugelman, J.R., Nyenswah, T.G., Ladner, J.T., Wiley, M.R., Cordier-Lassalle, T., Christie, A., Schroth, G.P., Gross, S.M., Davies-Wayne, G.J., Shinde, S.A., Murugan, R., Sieh, S.B., Badio, M., Fakoli, L., Taweh, F., de Wit, E., van Doremalen, N., Munster, V.J., Pettitt, J., Prieto, K., Humrighouse, B.W., Stroher, U., DiClaro, J.W., Hensley, L.E., Schoepp, R.J., Safronetz, D., Fair, J., Kuhn, J.H., Blackley, D.J., Laney, A.S., Williams, D.E., Lo, T., Gasasira, A., Nichol, S.T., Formenty, P., Kateh, F.N., De Cock, K.M., Bolay, F., Sanchez-Lockhart, M., Palacios, G., 2015. Molecular evidence of sexual transmission of ebola virus. N. Engl. J. Med. 373, 2448–2454.
Moller-Tank, S., Maury, W., 2015. Ebola virus entry: a curious and complex series of events. PLoS Pathog. 11, e1004731.
Mondor, I., Ugolini, S., Sattentau, Q.J., 1998. Human immunodeficiency virus type 1 attachment to HeLa CD4 cells is CD4 independent and gp120 dependent and requires cell surface heparans. J. Virol. 72, 3623–3634.
Nakayama, E., Yokoyama, A., Miyamoto, H., Igarashi, M., Kishida, N., Matsuno, K., Marzi, A., Feldmann, H., Ito, K., Saijo, M., Takada, A., 2010. Enzyme-linked immunosorbent assay for detection of filovirus species-specific antibodies. Clin. Vaccine Immunol. : CVI 17, 1723–1728.
Nanbo, A., Imai, M., Watanabe, S., Noda, T., Takahashi, K., Neumann, G., Halfmann, P., Kawaoka, Y., 2010. Ebolavirus is internalized into host cells via macropinocytosis in a viral glycoprotein-dependent manner. PLoS Pathog. 6, e1001121.
O'Hearn, A., Wang, M., Cheng, H., Lear-Rooney, C.M., Koning, K., Rumschlag-Booms, E., Varhegyi, E., Olinger, G., Rong, L., 2015. Role of EXT1 and glycosaminoglycans in the early stage of filovirus entry. J. Virol. 89, 5441–5449.
Odendall, C., Dixit, E., Stavru, F., Bierne, H., Franz, K.M., Durbin, A.F., Boulant, S., Gehrke, L., Cossart, P., Kagan, J.C., 2014. Diverse intracellular pathogens activate type III interferon expression from peroxisomes. Nat. Immunol. 15, 717–726.
Ohshiro, Y., Murakami, T., Matsuda, K., Nishioka, K., Yoshida, K., Yamamoto, N., 1996. Role of cell surface glycosaminoglycans of human T cells in human immunodeficiency virus type-1 (HIV-1) infection. Microbiol. Immunol. 40, 827–835.
Olejnik, J., Hume, A.J., Leung, D.W., Amarasinghe, G.K., Basler, C.F., Muhlberger, E., 2017. Filovirus strategies to escape antiviral responses. Curr. Top. Microbiol. Immunol. 411, 293–322.
Pinto, A.K., Williams, G.D., Szretter, K.J., White, J.P., Proenca-Modena, J.L., Liu, G., Olejnik, J., Brien, J.D., Ebihara, H., Muhlberger, E., Amarasinghe, G., Diamond, M.S., Boon, A.C., 2015. Human and murine IFIT1 proteins do not restrict infection of negative-sense RNA viruses of the orthomyxoviridae, bunyaviridae, and Filoviridae families. J. Virol. 89, 9465–9476.
Purpura, L.J., Soka, M., Baller, A., White, S., Rogers, E., Choi, M.J., Mahmoud, N., Wasunna, C., Massaquoi, M., Vanderende, K., Kollie, J., Dweh, S., Bemah, P., Christie, A., Ladele, V., Subah, O., Pillai, S., Mugisha, M., Kpaka, J., Nichol, S., Stroher, U., Abad, N., Mettee-Zarecki, S., Bailey, J.A., Rollin, P., Marston, B., Nyenswah, T., Gasasira, A., Knust, B., Williams, D., 2016. Implementation of a national semen testing and counseling program for male ebola survivors - Liberia, 2015-2016. MMWR. Morb. Mort. Weekly Rep. 65, 963–966.
Rhein, B.A., Powers, L.S., Rogers, K., Anantpadma, M., Singh, B.K., Sakurai, Y., Bair, T., Miller-Hunt, C., Sinn, P., Davey, R.A., Monick, M.M., Maury, W., 2015. Interferon-gamma inhibits ebola virus infection. PLoS Pathog. 11, e1005263.
Rodriguez, L.L., De Roo, A., Guimard, Y., Trappier, S.G., Sanchez, A., Bressler, D., Williams, A.J., Rowe, A.K., Bertolli, J., Khan, A.S., Ksiazek, T.G., Peters, C.J., Nichol, S.T., 1999. Persistence and genetic stability of ebola virus during the outbreak in kikwit, democratic republic of the Congo, 1995. J. Infect. Dis. 179 (Suppl. 1), S170–S176.
Rowe, A.K., Bertolli, J., Khan, A.S., Mukunu, R., Muyembe-Tamfum, J.J., Bressler, D., Williams, A.J., Peters, C.J., Rodriguez, L., Feldmann, H., Nichol, S.T., Rollin, P.E., Ksiazek, T.G., 1999. Clinical, virologic, and immunologic follow-up of convalescent Ebola hemorrhagic fever patients and their household contacts, Kikwit, Democratic Republic of the Congo. Commission de Lutte contre les Epidemies a Kikwit. J. Infect. Dis. 179 (Suppl. 1), S28–S35.
Saeed, M.F., Kolokoltsov, A.A., Albrecht, T., Davey, R.A., 2010. Cellular entry of ebola virus involves uptake by a macropinocytosis-like mechanism and subsequent trafficking through early and late endosomes. PLoS Pathog. 6, e1001110.
Salvador, B., Sexton, N.R., Carrion Jr., R., Nunneley, J., Patterson, J.L., Steffen, I., Lu, K., Muench, M.O., Lembo, D., Simmons, G., 2013. Filoviruses utilize glycosaminoglycans for their attachment to target cells. J. Virol. 87, 3295–3304.
Shieh, M.T., WuDunn, D., Montgomery, R.I., Esko, J.D., Spear, P.G., 1992. Cell surface receptors for herpes simplex virus are heparan sulfate proteoglycans. J. Cell Biol. 116, 1273–1281.
Simmons, G., Reeves, J.D., Grogan, C.C., Vandenberghe, L.H., Baribaud, F., Whitbeck,

J.C., Burke, E., Buchmeier, M.J., Soilleux, E.J., Riley, J.L., Doms, R.W., Bates, P., Pohlmann, S., 2003. DC-SIGN and DC-SIGNR bind ebola glycoproteins and enhance infection of macrophages and endothelial cells. Virology 305, 115–123.

Sissoko, D., Duraffour, S., Kerber, R., Kolie, J.S., Beavogui, A.H., Camara, A.M., Colin, G., Rieger, T., Oestereich, L., Palyi, B., Wurr, S., Guedj, J., Nguyen, T.H.T., Eggo, R.M., Watson, C.H., Edmunds, W.J., Bore, J.A., Koundouno, F.R., Cabeza-Cabrerizo, M., Carter, L.L., Kafetzopoulou, L.E., Kuisma, E., Michel, J., Patrono, L.V., Rickett, N.Y., Singethan, K., Rudolf, M., Lander, A., Pallasch, E., Bockholt, S., Rodriguez, E., Di Caro, A., Wolfel, R., Gabriel, M., Gurry, C., Formenty, P., Keita, S., Malvy, D., Carroll, M.W., Anglaret, X., Gunther, S., 2017. Persistence and clearance of Ebola virus RNA from seminal fluid of Ebola virus disease survivors: a longitudinal analysis and modelling study. Lancet Global health 5, e80–e88.

Slenczka, W., Klenk, H.D., 2007. Forty years of marburg virus. J. Infect. Dis. 196 (Suppl. 2), S131–S135.

Soka, M.J., Choi, M.J., Baller, A., White, S., Rogers, E., Purpura, L.J., Mahmoud, N., Wasunna, C., Massaquoi, M., Abad, N., Kollie, J., Dweh, S., Bemah, P.K., Christie, A., Ladele, V., Subah, O.C., Pillai, S., Mugisha, M., Kpaka, J., Kowalewski, S., German, E., Stenger, M., Nichol, S., Stroher, U., Vanderende, K.E., Zarecki, S.M., Green, H.H., Bailey, J.A., Rollin, P., Marston, B., Nyenswah, T.G., Gasasira, A., Knust, B., Williams, D., 2016. Prevention of sexual transmission of Ebola in Liberia through a national semen testing and counselling programme for survivors: an analysis of Ebola virus RNA results and behavioural data. Lancet Global health 4, e736–743.

Stoltz, M., Klingstrom, J., 2010. Alpha/beta interferon (IFN-alpha/beta)-independent induction of IFN-lambda 1 (interleukin-29) in response to Hantaan virus infection. J. Virol. 84, 9140–9148.

Subissi, L., Keita, M., Mesfin, S., Rezza, G., Diallo, B., Van Gucht, S., Musa, E.O., Yoti, Z., Keita, S., Djingarey, M.H., Diallo, A.B., Fall, I.S., 2018. Ebola virus transmission caused by persistently infected survivors of the 2014-2016 outbreak in West Africa. J. Infect. Dis. 218 (suppl_5), S287–S291. https://doi.org/10.1093/infdis/jiy280 218.

Subtil, F., Delaunay, C., Keita, A.K., Sow, M.S., Toure, A., Leroy, S., Msellati, P., Magassouba, N., Baize, S., Raoul, H., Ecochard, R., Barry, M., Delaporte, E., Etard, J.F., Postebogui Study, G., 2017. Dynamics of ebola RNA persistence in semen: a report from the postebogui cohort in Guinea. Clin. Infect. Dis. : Off. Publ. Infect. Dis. Soc. Am. 64, 1788–1790.

Tamhankar, M., Gerhardt, D.M., Bennett, R.S., Murphy, N., Jahrling, P.B., Patterson, J.L., 2018. Heparan sulfate is an important mediator of Ebola virus infection in polarized epithelial cells. Virol. J. 15, 135.

Trombley, A.R., Wachter, L., Garrison, J., Buckley-Beason, V.A., Jahrling, J., Hensley, L.E., Schoepp, R.J., Norwood, D.A., Goba, A., Fair, J.N., Kulesh, D.A., 2010. Comprehensive panel of real-time TaqMan polymerase chain reaction assays for detection and absolute quantification of filoviruses, arenaviruses, and New World hantaviruses. Am. J. Trop. Med. Hyg. 82, 954–960.

WHO, 2016. Interim Advice on the Sexual Transmission of the Ebola Virus Disease. http://www.who.int/reproductivehealth/topics/rtis/ebola-virus-semen/en/.

WHO, 2018. http://www.who.int/ebola/situation-reports/drc-2018/en/.

Wool-Lewis, R.J., Bates, P., 1998. Characterization of Ebola virus entry by using pseudotyped viruses: identification of receptor-deficient cell lines. J. Virol. 72, 3155–3160.

Zaneveld, L.J., Anderson, R.A., Diao, X.H., Waller, D.P., Chany, C., Feathergill, K., Doncel, G., Cooper, M.D., Herold, B., 2002. Use of mandelic acid condensation polymer (SAMMA), a new antimicrobial contraceptive agent, for vaginal prophylaxis. Fertil. Steril. 78, 1107–1115.

Zhang, X., Brann, T.W., Zhou, M., Yang, J., Oguariri, R.M., Lidie, K.B., Imamichi, H., Huang, D.W., Lempicki, R.A., Baseler, M.W., Veenstra, T.D., Young, H.A., Lane, H.C., Imamichi, T., 2011. Cutting edge: Ku70 is a novel cytosolic DNA sensor that induces type III rather than type I IFN. J. Immunol. 186, 4541–4545.